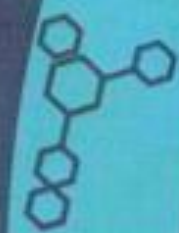# 7th

RCChE

2014 REGIONAL CONFERENCE ON CHEMICAL ENGINEERING

AUN SEED NET - Chemical Engineering

ABSTRACT BOOK

Strengthening Partnership to Enhance ASEAN's Industrial Competitiveness and Technology-Based Utilization of Natural Resources towards ONE ASEAN COMMUNITY

Melia Purosani Hotel, Yogyakarta, Indonesia

2 - 3 December 2014

Organized by

Supported by

AUN/SEED-Net

Chevron

VENUE

Melia Purosani Hotel
Jl. Suryotomo no 31 Yogyakarta 55122
Indonesia

INFORMATION

For further information please contact:

Chemical Engineering Department
Faculty of Engineering, Universitas Gadjah Mada
Jalan Grafika No. 2 Yogyakarta 55281, Indonesia

Account number: 137-00-1111512-4
an. SITI SYAMSIAH.RCEE2014
Bank : PT.Bank Mandiri Tbk Cabang Yogyakarta
Gd.Magister

Email: rcee2014@ugm.ac.id
Website: http://rcce2014.ft.ugm.ac.id

FLOW SHEET USER

USER → SIGN UP → SUBMISSION → EDIT ABSTRACT → Abstract Unaccepted / By Email / Abstract Accepted → UPLOAD FULL ARTICLE → EDIT ARTICLE → Article Unaccepted / By Email / Article Accepted → PAYMENT → ANNOUNCED TO PARTICIPANT LIST

CONTACT PERSON

Siti Syamsiah, PhD (Conference Chairman)
Chemical Engineering UGM
Phone. 62-274-902171 (office operator)
62-818270705 (mobile)
Fax. 62-274-902170 | 62-274-555321
Email. ssyamsiah@chemeng.ugm.ac.id

Wiratni, PhD (Conference Secretary)
Chemical Engineering UGM
Phone. 62-274-902171 (office operator)
62-81328183160 (mobile)
Fax. 62-274-902170 | 62-274-555321
Email. wiratni@chemeng.ugm.ac.id

2014 REGIONAL CONFERENCE ON CHEMICAL ENGINEER

"Strengthening Partnerships to Enhance ASEAN's Industrial Competitiveness and Technology-Based Utilization of Natural Resources towards ONE ASEAN COMMUNITY"

December, 2-3 2014
Melia Purosani Hotel
Yogyakarta Indonesia

Organized By:
Supported By:
KALBE

PROGRAM RUNDOWN

Tuesday, December 2, 2014	
Time	Agenda
08.00 – 08.20	Open registration desk
8.20 – 8.50	1. Opening Ceremony (MC) 2. Welcoming remark from Organizing Committee 3. Opening Addresses by JSUs, JICA, His 4. Welcoming remark by UNRI Rector 5. Official Opening by UGM Rector
08.50 – 09.00	Traditional welcoming dance by UGM student
09.00 – 10.30	**Plenary Panel I** **Advance topics in natural resources technology** 1. Professor Hirofumi Hinode (Tokyo Institute of Technology Japan) 2. Professor Hajime Tamon (Kyoto University Japan) 3. Professor Tatsuya Okubo (University of Tokyo) 4. Professor Luis Razon (De La Salle University – The Philippines)
10.30 – 10.45	Morning Coffee
10.45 – 12.00	**Plenary Panel II** **ASEAN Industrial Challenges: Innovation, Technology, and Sustainability** 1. General Manager on Technology and Product Development for PT. Pertamina Gas Directorate, 2. Direktur R & D PT. Soho Farmasi Industri 3. Pusat Penelitian Kelapa Sawit Medan
12.00 – 13.00	Lunch Break
13.00 – 15.00	- **Technical Sessions I** (up to 7 parallel rooms) - Field Management Meeting for JSUs and MIs
15.00 – 15.30	Afternoon Coffee
15.30 – 17.30	**Technical Sessions II** (up to 7 parallel rooms)
19.00 – 21.00	Collegial Banquet and Award Ceremony

Wednesday, December 3, 2014	
Time	Agenda
08.00 – 08.15	Registration
08.15 – 08.20	Opening salutation
08.20 – 10.00	**Plenary Panel III:** **Chemical Engineering Education Challenges and Opportunities** 1. Chairman of Indonesian Association of Chemical Engineering Profession (BKKPII) 2. The Former Rector of ASEAN Institute of Technology (AIT), 3. Chairman of Chemical Engineering Department, Universiti Malaya, Malaysia
10.00 – 10.15	Morning Coffee
11.15 – 11.45	**Information from AUN/SEED-Net secretariat about development of program**
11.45 – 12.00	Farewell Address to Foreign Delegations by Chemical Engineering UGM Chairman
12.00 – 13.00	Lunch
13.00 – night	City Tour

TECHNICAL SESSION

TECHNICAL SESSIONS I (13.00 – 14.30)

Room I (ARIMBI ROOM, Ground Floor)
Moderator : Yano Surya Pradana

Time	Code	Title	Presenter
13.00	M-05	Oil Palm Fruit Bunch Fibre Conversion to High Refined Cellulose Using Nitric Acid and Sodium Hydroxide as The Delignificating Agents	Supranto
13.15	M-04	Synthesis of Pumice-TiO_2 Composite for Phenol and E.Coli Removal	Hendarsa, Agung Sri
13.30	M-07	Flas'on (Fly Ash as Sound Absorbent Concrete): Production Sound Absorbent Concrete for Solve Noise Problem in Industrial Area	M Dwiki
13.45	M-08	Silica Gel Derived from Palm Oil Mill Fly Ash	Panca Setia Utama
14.00	M-09	Effect of Anodization Time and Temperature on The Morphology of TiO_2 Nanotube Arrays for Photocatalytic Hydrogen Production from Glycerol-Water Solution	Ratnawati
14.15	M-12	The Crystalline Phase and Particle Size of $NaTaO_3$ Nanomaterials Synthesized by Hydrothermal Method	Nguyen Thi Lan

TABLE OF CONTENTS

Effect of Anodization Time and Temperature on the Morphology of TiO₂ Nanotube Arrays for Photocatalytic Hydrogen Production from Glycerol Solution

Ratnawati[1], Jarnuzi Gunlazuardi[2], Slamet[1]

[1]Department of Chemical Engineering, Faculty of Engineering, Universitas Indonesia, Depok 16424, Indonesia, Tel.: +62-21-7863518, fax: +62-21-7863515,
[2]Department of Chemistry, Faculty of Mathematics and Sciences, Universitas Indonesia, Depok 16424, Indonesia, Tel.: +62-21-7270027, fax: +62-21-7863432,
Email: rnwt63@yahoo.co.id, slamet@che.ui.ac.id, jarnuzi@ui.ac.id

Abstract. Effect of anodization time and temperature on the morphology of TiO₂ nanotube arrays (TNTAs) photocatalyst and its application for H₂ production from glycerol-water solution has been investigated. The TNTAs were synthesized by anodic oxidation of titanium metal in glycerol electrolyte solution containing NH₄F, at 30 V with magnetically stirring. Annealing of the formatted TNTAs were performed at 500 °C for 3 hours under H₂in an argon atmosphere, to produce crystalline phase photocatalyst. FESEM   analysis showed that up to around 1.57 μm, self-organized and well ordered TNTAs have range of inner diameters and wall thicknesses approximately 67-205 nm and 10-30 nm respectively. Increasing the tube length (as a result of longer anodization time up to 6 hours), produced TNTAs with morphology disintegration. TNTAs synthesized at 50 °C for 1-6 hours anodization time produced TNTAs with length of the tube around 0.8–1 μm. It was found that the inner diameter value of the TNTAs increasing as anodization time increase across the range of 1-6 hours and the temperature increase from 28 to 50 °C. Photocatalytic H₂ production indicated that accumulative H₂ generation was found to depend on the tube dimension and the morphology of TNTAs as those factors would influence photon absorption. For the TNTAs synthesized at 28 °C for 2 hours, FTIR analysis indicated that C and N were incorporated into the TNTAs lattice. As a result, this TNTAs has the band gap of 2.7 eV, with anatase phase. Photocatalytic H₂ production test indicated that this photocatalyst showed higher H₂ production compare to other conditions and can be considered as the optimum condition.

Key Words: *Annealing; Anodization; Hydrogen; Magnetic stirring; Photocatalytic; TiO₂ Nanotube Arrays.*

1   Introduction

Sustainable energy and environmental issues are two concern factors in recent society. Nowadays, the major source of energy is fossil fuels and its combustion cause pollution. Hydrogen as renewable and clean energy is an important alternative due to increasing global energy demand (especially in fuel cell), inevitable depletion of fossil fuels and environmental problems [Haifeng et al, 2013]. Among various routes for hydrogen production, the photocatalytic splitting of water over TiO₂ has been considered as a promising alternative technology [Haifeng et al, 2013, Rajini et al, 2012]. Whereas, the biomass-derived waste such as glycerol solution (by-product of the biodiesel industry that now has limited demand in the market) [Vasileia and Demitris, 2009], presents a particularly attractive renewable and sustainable source for H₂ generation. Glycerol solution gives some advantages since it serves as a hydrogen source, and as a sacrificial agents/electron donor in water splitting, which can increase the H₂ produced from both kinetic and thermodynamic points of view [Slamet et al, 2013]. Therefore, this would be beneficial as a new renewable source for the H₂ production and waste minimization. TiO₂

is the most promising candidate photocatalyst due to its photostability, environmental harmlessness, non-toxicity, availability, relatively inexpensive and has powerful oxidation properties [Haifeng et al, 2013]. Activation of TiO_2 needs photon energy, whichcan be provided by solar light at ambient condition instead of thermal energy [Wang et al, 2009]. One of the TiO_2 applications is photocatalyst in H_2 generation [Slamet et al, 2013, Ratnawati et al, 2014], and it is commonly used as a semiconductor in photo-spitting of water. However, its application has several drawbacks due to rapid recombination of photoinduced electron-hole [Haifeng et al, 2013, Rajini et al, 2012], limited surface area and visible light inactive (its wide band gap i.e. 3.2 eV for the anatase and 3.0 eV for rutile phase) [Xi et al, 2013]. Consequently, its utilization efficiency especially in solar light is still poor as UV portion accounts for only about 5%, meanwhile visible light accounts for about 45% in solar spectra [Susanta et al, 2007]. Therefore, some modifications strategies need to be done to reduce those drawbacks such as morphology modifications [Haifeng et al, 2013 , Rajini et al, 2012, Wang et al, 2009], non-metal (C,N, B) and metal (Pt, Cu) doping [Haifeng et al, 2013 , Slamet et al, 2013, Wang et al, 2009, Na et al, 2008, Muhammed and Rohani, 2011].

Many strategies have been proposed to enhance photoactivity of TiO_2 is synthesizing it to get morphology modifications in the forms of nanotubes. It was reported that TiO_2nanotube arrays (TNTAs) morphology, obtaining by anodic process of titanium metal, has performed better properties as it provides a larger surface area compare to random nanoparticle [Xi et al, 2013, Susanta et al, 2007]. In synthesizing TNTAs by anodization process, anodization time and temperature affect the dimension and morphology of TNTAs produced [Wen-Yu and Bo Ruei, 2013]. In this study, the investigation of those effects on morphology of TNTAs and its activity under visible light illumination in producing H_2 from photo-reforming of glycerol solution (10 vol% of glycerol) was performed.

2 Methodology

### 2.1.Materials.

All chemicals were purchased from commercial source and used without further purification: HF (Merk, 40%), HNO_3 (Merk 65%), NH_4F (Merck, 98%), Glycerol (technical grade, 98,8%), TiO_2 P-25, 20% H_2/Ar and Argon (99,9%). Material for anodization: Ti foil as anode (99,6% purity, thick 0.3 mm) dan Pt as cathode (thick 1 mm). All solutions were prepared using purity DI water.

2.2. Synthesis of TNTAs

Titanium foils were used as a substance for the growth of TNTAs. Prior to anodization, the Ti sheets were first mechanically polished with a 1500 cc sand paper, degreased in a mixture of HF, HNO_3 and H_2O, rinsed in deionized water and dried under air. TNTAs were obtained by the anodic oxidation process which performed in a two electrode configuration with a Ti foil as an anode and a platinum, Pt as a cathode. The distance between the two electrodes was kept at 3.5 cm in all experiments. A constant of 30 V potential difference was set by power supply (Escord 6030SD). To study the effect of anodiation time and temperature, the anodization times were varied from 1 to 6 hours, and the temperatures were set around 28 and 50 °C. Magnetically stirring was done in the anodization process.

The glycerol solution containing 0.5 wt.% NH$_4$F with water content of 25 v% was used as the electrolyte solutions. The formatted TNTAs were washed in distilled water, dried under air atmosphere and subsequently annealed to convert the amorph phase to the anatase phase using 20% hydrogen in an argon atmosphere at 500 ^{o}C with the rate of 150 ml s^{-1} in a furnace. The temperature of the furnace was raised to 500 ^{o}C, held for 3 hours and cooled naturally to room temperature. The schematic of anodization of Ti can be seen in Fig. 1.
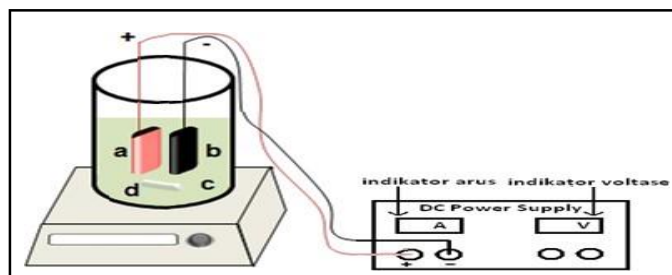
Figure 1 The schematic of anodization process with (a) Ti foil (anode), (b) Pt (cathode), (c) electrolyte solution and (d) magnetic bar

2.3. Characterization of TNTAs

The morphology/tube dimension of TNTAs was characterized using Field Emission Scanning Electron Microscopy (FESEM, FEI-Inspect F50) with accelerating voltage of 20 kV. The energy-dispersive X-ray spectroscopy (EDS) which is attached to the SEM was done to analyze the elemental composition. FTIR spectra were recorded using Shimadzu IR Prastige-21 (wave number range of 400-4000 cm^{-1}) and it was used for analyzing the functional groups present in the TNTAs. A UV-Vis Spectroscopy (DRS) spectra of TNTAs samples were measured using spectrophotometer Shimadzu 2450 type. The spectra of the samples were recorded under ambient condition in the wavelength range of 200-900 nm, and this analysis was also carried out to calculate the energy band gap. To evaluate the crystalline phase of the TNTAs, X-ray diffraction (XRD) analysis (Shimadzu 7000 X-ray diffractometer) was performed. The source of the X-ray radiation was Cu Kα ($\lambda = 0.154184$ nm) over the 2θ range of 10–80° with the scan rate 2° min^{-1} while the accelerating voltage and the applied current were 40 kV and 30 mA, respectively. The Scherrer equation is used to estimate the crystallite sizes of the sample from FWHM (full-width at half-maximum) of XRD. Photocurrent density measurements were performed in the photoelectrocatalytic reactor with a standard three-electrode configuration in with TNTAs (photoanode), a Pt wire and a saturated Ag/AgCl as working, counter and reference electrodes, respectively. All three electrodes in the reactor were connected to a computer - controlled potentiostat (Edaq/e-corder 401) to record the photocurrent generated and 0.1 M NaNO$_3$ as supporting electrolyte.

2.4. Photocatalytic hydrogen production

Experiments on H$_2$ generation were performed via photocatalytic reaction. The reaction was carried out in a 500 ml Pyrex glass reactor equipped with a mercury lamp of Philips HPL-N 250 as a photon source (17% of UV and 83% of visible light), thermocouple and magnetic stirrer. The lamp was positioned one cm away from the reactor as a photon source. The photoreactor system was placed inside a reflector box, and the reactions were carried out for 4 hours irradiation as shown in Fig. 2. Before irradiation, argon was introduced into the reactor system for purging and high purity argon (99.9%) is used as a

carrier gas. The H_2 produced was analyzed by on-line sampling every 30 min using Shimadzu Gas Chromatograph (GC 2014) equipped with Thermal Conductivity Detector (TCD). Molecular sieve (MS Hydrogen 5A, 80-100 mesh) column was used for H_2 analysis, respectively. A schematic diagram of the photocatalytic reactor is presented in Fig. 2.


Argon   Argon
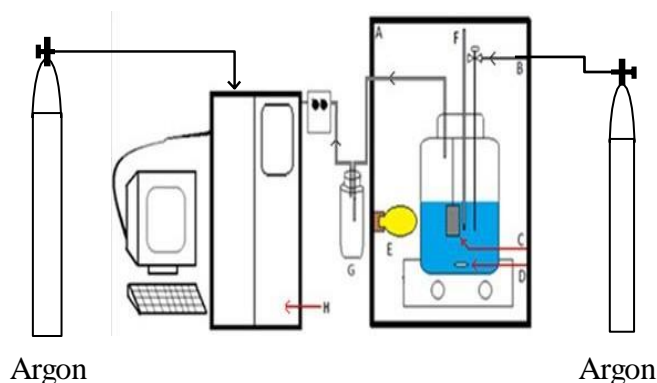
Figure 2 Schematic diagram of the photocatalytic reactor: (A) reflector box, (B) line purging, (C) photocatalyst, (D) magnetic stirrer, (E) mercury lamp, (F) thermocouple, (G) liquid condensation tube and (H) GC

3   Results and Discussion
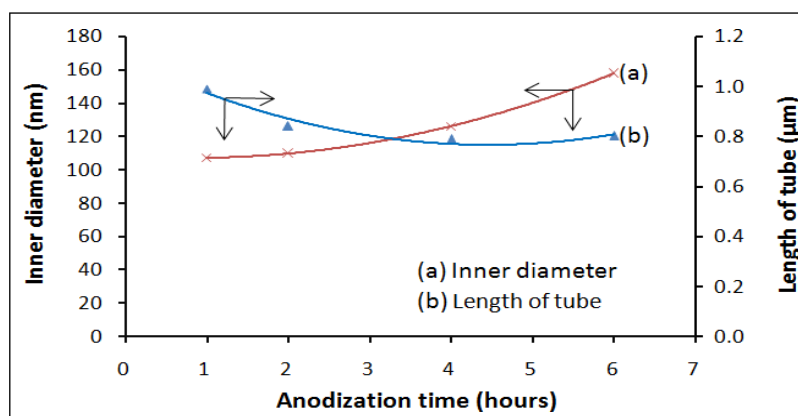
3.1. Effect of anodization time

Fig. 3 shows FESEM top and cross section view image (inset in Fig. 3) of TNTAs with 1; 2; 4; dan 6 hours at 50 °C, whereas Fig. 4 shows view image with angle 45°. The effect of the anodization time on the dimension of TNTAs produced can be seen in Table 1 and Fig. 5.
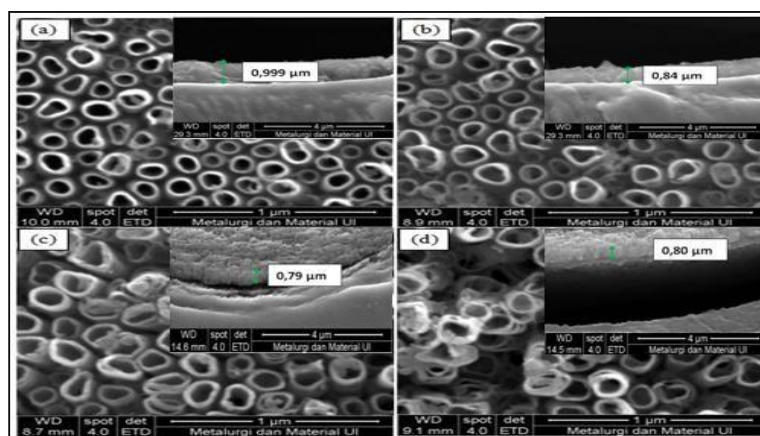
Figure 3 FESEM top and cross section view image (inset) of TNTAs prepared by anodization at 50 °C for (a) 1, (b) 2, (c) 4 (d) 6 hours
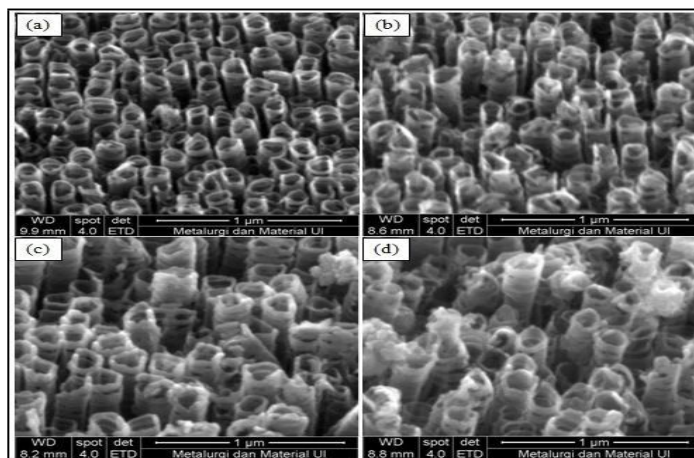
Figure 4 FESEM top view image with angle 45 º of TNTAs prepared by anodization at 50 ºC for (a) 1, (b) 2, (c) 4 and (d) 6 hours

Figure 5 The effect of anodization time on the inner diameter and the tube length of TNTAs at 50 ºC

As shown in Fig. 4 and 5, the inner diameter of the TNTAs increase as anodization time increase across the range of 1-6 hours, however, the tube length decrease and then achieve constant condition. Furthermore, with increasing time, some of the TNTAs were collapse, dissolved, and the tube length became ununiform (Fig. 3 and 4). The formation mechanism of the TNTAs from Ti can be explained as follows [Muhammed and Rohani, 2011].

$$2H_2O \rightarrow 2[O] + 4e^- + 4H^+ \tag{1}$$

$$Ti + 2[O] \rightarrow TiO_2 \tag{2}$$
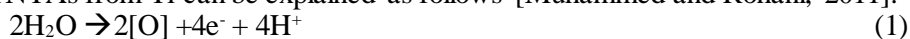
The overall reaction become:

$$Ti + 2H_2O \rightarrow TiO_2 + 4H^+ + 4e^- \tag{3}$$

The formation of small pits or pores due to H^+ and F^- ions given by the reaction:

$$TiO_2 + 6 F^- + 4H^+ \rightarrow (TiF_6)^{2-} + 2H_2O \tag{4}$$
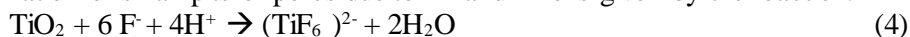
In the cathode (Pt), the reduction reaction of H^+ take place and the H_2 was formed

$$4H^+ + 4e^- \rightarrow 2H_2 \tag{5}$$
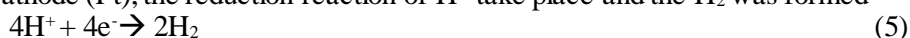
Firstly, Ti surface is oxidized to form TiO_2 layer according to the (Eq.3) and followed by dissolution of TiO_2 (electric field-assisted oxidation and dissolution), therefore, tube-like TiO_2 layer was obtained. Ti and TiO_2 are also chemically dissolved since the availability of fluoride and acidic environment according to (Eq.4). The chemical dissolution process happens at the entire porous surface. The dissolution of the TNTAs in the bottom and the wall of the tube resulted in the longer the tube length and wider the inner diameter. However, the dissolution in the mouth resulted in the shorter the tube length. In the first hour, the formation of the TNTAs in fast speed, therefore around 1 μm length of TNTAs was achieved (Table 1 and Fig.4). With increasing the time of anodization, the oxidation and dissolution slowed down (due to high electric resistance by thicker oxide layer and long diffusion of F^+ to the bottom of the tube) caused the formation and dissolution of the TNTAs reached equilibrium. Finally, the dissolution in the mouth was little faster than the oxidation and dissolution in the bottom of the tube, resulted in the shorter the tube length [Lei et al, 2010].

The tube dimension is a result of the competition of the oxidation and dissolution of the TNTAs, and therefore any variation affecting these processes such as anodic voltage, reaction time, reaction temperature, pH value and so on [Wen-Yu and Bo-Ruei, 2013, Lei et al, 2010]. From these results, the maximum length of the TNTAs was reached at 1 hour anodization and hereafter the equilibrium was achieved. In addition, the collapse of the tube was obtained. This phenomenon is predicted that at 50 °C anodization temperature with magnetically stirring caused faster movement of H^+, F^- and (or TiF^6) in the electrolyte [Lei et al, 2010]. As a result, this situation affects the dimension, morphology of the TNTAs and a faster equilibrium occurred. This result is in agreement with Yu Wang W. and Ruei Chen B., 2013. They reported that collapse and decrease of the nanotube length was occured with increasing the time of anodization (with the anodization condition: 40 °C, without magnetically stirring, 30 V and weight ratio of glycerol to water 6:4). In this study, until 6 hours anodization, the inner diameter increased (resulted from the dissolution to the wall) but partly of the tube were collapse. The ununiform in the length tube with increasing the time is predicted by the longer of time of magnetically stirring during the anodization.

Fig. 6 shows accumulative H_2 production (μmol/cm^2 of photocatalyst) from glycerol solution as a function of irradiation time on TNTAs with various of anodization time. Photocatalytic production of H_2 from glycerol-water mixture consists of two distinct mechanisms namely photo-spitting of water (at glycerol concentration of 0%) and photo-reforming of glycerol [Slamet et al, 2013]. In photo-splitting of water, hole oxidizes water to produce $\cdot OH$ and H^+ according to Eq.(7), and then H^+ undergoes reduction with electron to produce H_2 (Eg. (8)).

$$TiO_2 + hv \rightarrow TiO_2(h^+ + e^-) \tag{6}$$
$$h^+ + H_2O \rightarrow \cdot OH + H^+ \tag{7}$$
$$H^+ + e^- \rightarrow 0.5H_2 \tag{8}$$

In photo-reforming of glycerol, it is oxidized by hole, $\cdot OH$ and/or oxygen produced by cleavage of water to produce several intermediate compounds followed by H_2 and CO_2 generation as the end product [Vasileia and Demitris, 2009]. The two reactions (photo-spitting of water and photo-reforming of glycerol) take place simultaneously, and the combination of those reactions called as glycerol steam photo-reforming according to the overall reaction as follows [Vasileia and Demitris, 2009, Slamet et al, 2013]:

$$C_3H_8O_3 + 3H_2O \rightarrow 3CO_2 + 7H_2 \tag{9}$$
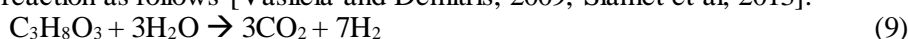
Therefore, introducing glycerol in the reactant could improve H_2 production as glycerol can act as sacrificial agents/hole scavenger that able to reduce the electron-hole recombination and as hydrogen source/reactant that undergoes oxidation reaction [Vasileia and Demitris, 2009, Slamet et al, 2013].

As presented in Fig. 6, it is obvious that, the hydrogen generation with TNTAs produced in 1; 2; 6 and 6 hours anodization time relatively constant as the length of the TNTAs also relatively similar. In photocatalytic reaction on the surface of TNTAs, the length of the tube proportional to photon absorbtion and therefore comparable with the H_2 production. Index 1; 2; 4 and 6 indicated the anodizatin time is performed in 1; 2; 4 and 6 hours).
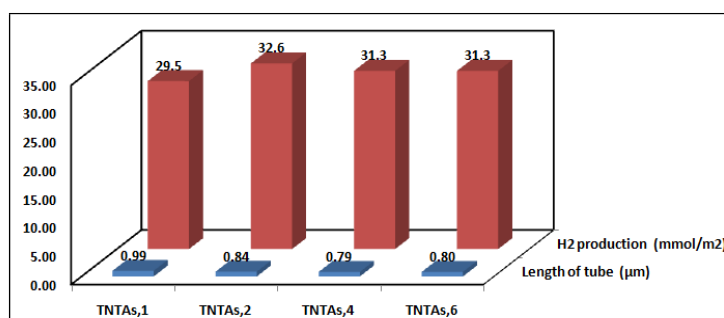

Figure 6 H_2 production for 4 hours irradiation and tube length of TNTAs as a function of anodization time

3.1 Effect of anodization temperature

To study the effect of anodization temperature, Fig. 7 shows FESEM image with angle 45° of TNTAs prepared by anodization for 2 hours at 28 and 50 °C, whereas Fig. 8 performs the FESEM images with angle 45 ° of TNTAs prepared by anodization for 6 hours at 28 and 50 °C. The summary of the tube size of TNTAs and H_2 production is presented in Table 1.
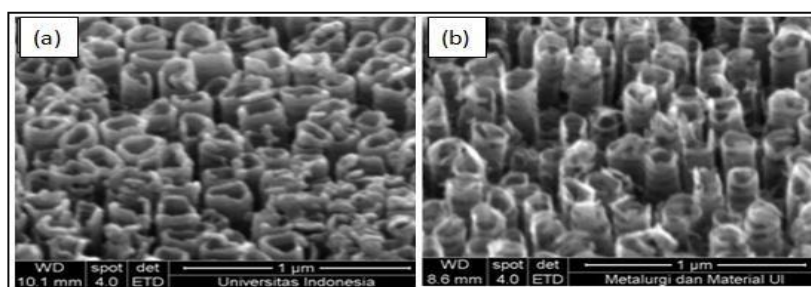
Figure 7 The FESEM top images with angle 45 ° of TNTAs prepared by anodization for 2 hours at (a) 28 °C and (b) 50 °C.
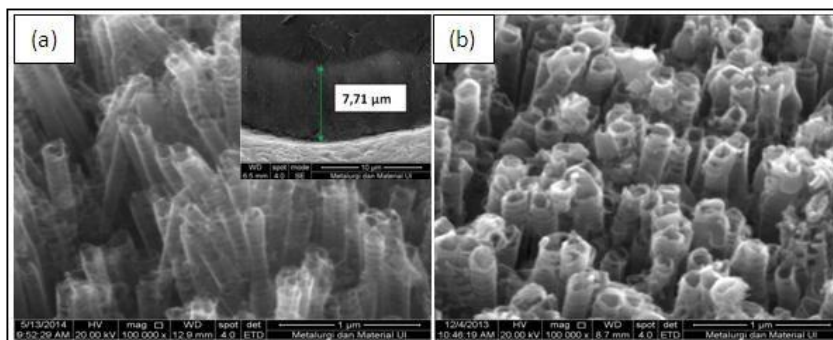
Figure 8 The FESEM images with angle 45 º of TNTAs prepared by anodization for 6 hours at (a) 28 ºC and 50 ºC

Tabel 1 Tube size of TNTAs and H_2 production

Anodizaion time, hour	Anodization Temperatur 28^{0}C				Anodization Temperature 50 ^{0}C			
	Di^a, nm	t^b, nm	L^b, μm	H_2^c, mmol/m^2	Di, nm	t, nm	L^b, μm	H_2^c, mmol/m^2
2	96	27	1.570	47.0	107	19	0.84	32.6
6	105	20	7.707	37.2	158	23	0.80	31.3

Di^a = average inner diameter, t^b= average thickness , L^b = average length , H_2^c = H_2 production

As shown in Table 1, It was found that with the temperature and time anodization increase, the inner diameters value of TNTAs increase since dissolution to the tube wall increase. However, the thickness the tubes are relatively constant. The difference of the TNTAs dimension is caused by the competition of the oxidation reaction of Ti to TiO_2 and chemical dissolution of formed TiO_2 that is influenced by time and temperature of anodization. At 28 ºC anodization temperature, the length of TNTAs increased from 1.57 up to 7.707 μm when the anodization time increased from 2 to 6 hours. Although longer of TNTAs produced at 6 hours anodization, disorder or ununiform of the tube length were observed (Fig. 8 and 9). Furthermore, length of the tube consists of layers of the tube (be in piles) as presented in Fig. 9. This finding is predicted influenced by longer anodization time (6 hours). While at 50 ºC anodization temperature, the length of TNTAs were relatively constant although the anodization time increased as an equilibrium reaction (the oxidation and dissolution) has achieved quickly and after that there is no addition length was observed.
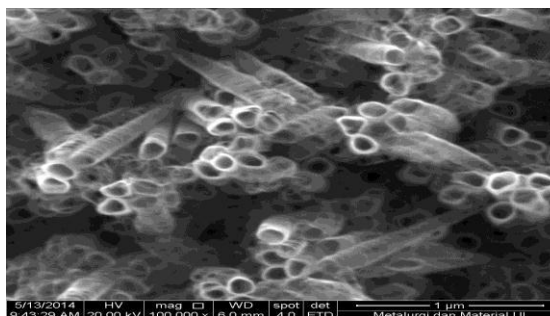
Figure 9 The FESEM images of TNTAs prepared by anodization for 6 hours at 28 oC

The tube dimension and the morphology of TNTAs influence the photon absorption and consequently affect the hydrogen production as can be seen in the Table 1 column 5 and 9. The TNTAs obtained for 6 hours anodization time at 28 °C with the tube length of 7.707 μm, H_2 produced was 37.2 mmol/m^2 TNTAs. In contrast, 6 hours anodization time, at 50 °C with the tube length 0.80 μm produced 31.3 mmol/m2 TNTAs. This condition occurred since the morphology of TNTAs with the length 7.707 μm (resulted from long anodization time) consisted of layers of the tube (be in piles) with disorder morphology (nanotube non array) that influence the photon absorption. Another possibility is longer TNTAs caused photon penetration did not reach the tube bottom. Among all of the TNTAs produced, TNTAs synthesized in 2 hours at room temperature showed highest photocatalytic hydrogen production (47.0 mmol/m2) from 10 %v glycerol-water solution and can be considered as the optimum condition.

For the TNTAs synthesized at room temperature (28 °C) with 2 hours anodization, the EDX analysis indicated that in addition to Ti and O, the C, N and F were also observed. When anodization process the glycerol and NH_4F were decomposed and glycerol as a carbon source and NH_4F as N and F source. Annealing with H_2/Ar leads to internal diffusion of C, N and F into TNTAs lattice. Therefore, FTIR analysis indicated that C and N were incorporated into the anatase TNTAs lattice (Fig.10). Peak at around 1050 cm^{-1} and around 1200 cm^{-1} are assigned for N-Ti-O bond and Ti-O-C bonds [Yean and Ahmad, 2013 ,Parra et al, 2008]. As a result, the band gap was observed decreasing to as low as 2.7 eV (Fig. 11). Therefore, this TNTAs provided current density of 0.086 mA/cm^2 at 1 V vs. Ag/AgCl) when it was illuminated with a tungsten lamp (350-800 nm) in photoelectrocatalytic test.
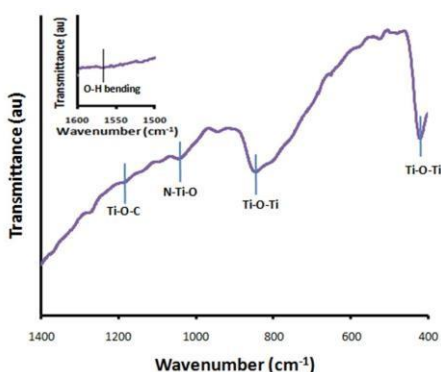
Figure 11 FTIR Spectra of TNTAs
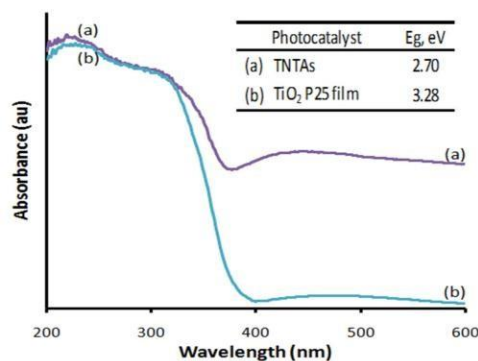
Figure 12 DRS Spectra of TNTAs

4   CONCLUSIONS

In summary, TNTAs films were synthesized using anodization method in glycerol electrolyte containing NH_4F with magnetically stirring. The inner diameter of the TNTAs increased as anodization time and temperature risen. At 28 °C anodization temperature, the length of TNTAs increased when the anodization time increased, while at 50 °C, the length of TNTAs were relatively constant although the anodization time increased (1-6 hours). Partially disorder and cluster of TNTAs was observed when TNTAs was synthesized at 28 °C for 6 hours as too long anodization time with magnetically stirring. The difference of the TNTAs morphology is caused by the competition of the oxidation reaction of Ti to TiO_2 and chemical dissolution of formed TiO_2 that is influenced by time and temperature of anodization. With the H_2 production, it was found that that TNTAs synthesized in 2 hours at 28 °C showed well-defined, highly ordered, and uniformed TNTAs with highest photocatalytic hydrogen production from 10 %v glycerol-water solution and can be considered as the optimum condition. The higher the temperature up to 50 °C and the longer anodization time (up to 6 hours), the bigger the inner diameter of TNTAs. However, tube length was found ununiform. Anodization time and temperature determine when the equilibrium (the oxidation and dissolution reaction) take place.

5   REFERENCES

[1]   Haifeng D, Xinfa D, Yingchao D, Yan Z, Stuart H. (2013) TiO_2 nanotubes coupled with nano-$Cu(OH)_2$ for highly efficient photocatalytic hydrogen production. Int J Hydrogen Energy;38:2126-35.

[2]   Lei H, Feng P, Hao Y, Hongjuan W, Jian Y, Zhong L. (2010) The influence of ultrasound on the formation TiO_2 nanotube arrays. Materials Research Bulletin;45:200-204

[3]   Muhamed AER, Rohani S. (2011) Modified TiO_2 nanotube arrays (TNTAs): progressive strategies towards visible light responsive photoanode, a review. Energy Environ Sci ;4:1065-86

[4]   Na L, Huimin Z, Jingyuan L, Xie Q, Shuo C. (2008) Characterization of boron-doped TiO_2 nanotube arrays prepared by electrochemical method and its visible light activity. Sep Purif Technol;62:668-73.

[5]   Parra R, Goes MS, Castro MS, Longo E, Bueno PR, Varela JA. (2008) Reaction pathway to the synthesis of anatase via the chemical modification of titanium isopropoxide with acetic acid. Chem Mater;20:143-150

[6]   Rajini PA, Tom M, C. Ramesh, M Murugesan, Arup D, S Dhara et al. (2012) Efficient photocatalytic hydrogen generation by Pt modified TiO_2 nanotubes fabricated by rapid breakdown anodization. Int J Hydrogen Energy;37:8268-76.

[7]   Ratnawati, Jarnuzi G., Eniya L. D., Slamet. (2014) Effect of $NaBF_4$ addition on the anodic synthesis of TiO_2 nanotube arrays photocatalytic for production of hydrogen from glycerol-water solution. Int J Hydrogen Energy;39:16927-16935

[8]   Slamet, Dewi T, Valentina, Muhammad I. (2013) Photocatalytic hydrogen production from glycerol-water mixture over Pt-N-TiO_2 nanotube photocatalyst. Int. J Energy Res, 37:1372-81.

[9]   Susanta KM, Mano M, Vishal KM, Krishnan SR. (2007) Design of a highly efficient photocatalytic cell for hydrogen generation by water splitting: Application of $TiO_{2-x}C_x$ nanotube as a photoanode and Pt/TiO_2 nanotube as a cathode. J Phys Chem C ;111:8677-85.

[10] Vasileia MD, Demitris IK. (2009) Efficient production of hydrogen by photo-induced reforming of glycerol at ambient conditions. Catal Today;144:75-80.

[11] Wang, WC, Liu CH, Liu CW, Chao JH, Lin, CH. Effect of Pt loading order on photocatalytic activity of Pt/TiO$_2$ nanofiber in generation of H$_2$ from neat ethanol. (2009) J Phys Chem C;113:13832-40.

[12] Wen-Yu W, Bo-Ruei C. Characterization and Photocatalytic Activity of TiO$_2$ Nanotube Films Prepared by Anodization. (2013) Int J of Photoenergy;2013:1-12

[13] Xi P, Qin X, Wu-lin C, Gui-lin Z, Xing Z, Jian-guo W. Tuning the catalytic property of TiO$_2$ nanotube arrays for water splitting. (2013) Int J Hydrogen Energy;38:2095-105.

[14] Yean LP, Ahmad ZA. (2013) Effect of carbon and nitrogen co-doping on characteristics and sonocatalytic activity of TiO$_2$ nanotube TNT for degradation of Rhodamine B in water. Chem Eng J;214:129-38.